On the Identity of the Last Known Stable Radical in X-irradiated Sucrose

Jevgenij Kusakovskij[a], Hendrik De Cooman[a], Einar Sagstuen[b], Freddy Callens[a], Henk Vrielinck[a,*]

[a]*Department of Solid State Sciences, Ghent University, Krijgslaan 281-S1, 9000 Ghent, Belgium*
[b]*Department of Physics, University of Oslo, P.O. Box 1048 Blindern, 0316 Oslo, Norway*

Abstract

Identification of radiation-induced radicals in relatively simple molecules is a prerequisite for the understanding of reaction pathways of the radiation chemistry of complex systems. Sucrose presents an additional practical interest as a versatile radiation dosimetric system. In this work, we present a periodic density functional theory study aimed to identify the fourth stable radical species in this carbohydrate. The proposed model is a fragment suspended in the lattice by hydrogen bonds with an unpaired electron at the original C5' carbon of the fructose unit. It requires a double scission of the ring accompanied by substantial chemical and geometric reorganization.

Keywords: density functional theory, ionizing radiation, radicals, sucrose

1. Introduction

Sucrose ($C_{12}H_{22}O_{11}$) can be found in almost every household as the main constituent of table sugar, as a sweetener in foodstuffs or as a component of medication [1]. Accidental or intentional exposure of this disaccharide to ionizing radiation leads to formation of free radicals. Knowledge of the radical composition permits mapping of chemical reaction pathways, which may be of interest for future drug design and food processing techniques. Studies of the radical catalysis of biomass sugars are also likely to benefit from this knowledge [2, 3, 4]. In its pure form, sucrose is considered to be an interesting solid state electron paramagnetic resonance (EPR) dosimetric system with a broad range of potential applications [5, 6, 7]. Despite all of the advantages of sucrose, like a considerable linear dose response and a relatively low detection limit, the multicomponent nature of its radiation-induced EPR spectrum has slowed down further improvement of dose assessment protocols. A complete understanding of the spectrum may improve this situation.

For the aforementioned reasons, considerable effort has been devoted to identifying stable and unstable radicals in irradiated sucrose using EPR spectroscopy data. The stable

---

*Corresponding author
Email address: Henk.Vrielinck@UGent.be (Henk Vrielinck)

spectrum of irradiated sucrose has been known for almost sixty years [8], but systematic studies directed at determining chemical structures were started only in the late eighties [9]. In the course of the last decade, the presence of four different species was established. All of them were thoroughly characterized using electron-nuclear double resonance spectroscopy (ENDOR) and three out of four were convincingly identified by comparing experimental **g** and hyperfine coupling (HF) tensors with density functional theory (DFT) calculations [10, 11, 12, 13]. For convenience, chemical structures of these radicals are presented in Fig. 1 together with a pristine sucrose molecule and the labeling scheme. In all previous studies, ENDOR characterization was performed at 110 K several days after room temperature (RT) irradiation. (For a thorough discussion of the topic, the reader is referred to Ref. 14.) In the present contribution, we propose and validate a model for the last unidentified stable radical species. It is demonstrated that the unpaired electron density is centered close to the pristine C5' site in the fructose unit and implies rather intricate rearrangements of the host molecule, resulting in an isolated radical fragment, suspended by hydrogen bonds in the lattice. Calculations based on the proposed model fit the experimental data remarkably well, which strongly suggests that the model is correct. This completes our understanding of the dominant stable radical structures formed in crystalline sucrose by X-irradiation.

2. Computational Methods

Periodic DFT calculations were employed to test radical models, devised from the experimental data [13] and solid-state radiation chemistry principles. The calculation methodology has been developed and validated in other studies on various carbohydrates and amino acids [14, 15, 16]. The model validation procedures rely on a comparison of experimental **g** and HF tensors to calculated ones. For a given pair of tensors, agreement is considered very good if deviation angles between their principal directions are of the order of 10° or less, the anisotropy of principal values is reproduced and the isotropic parts coincide within an accuracy of about 15%. In principle such agreement could be further improved for specific systems by fine tuning the level of theory, i.e. the basis set and the functional, but this would trade off the generality of the approach.

The crystal structure of sucrose is monoclinic with space group $P2_1$. This implies two molecules in a unit cell related by a twofold screw axis ($<b>$). All tensors are presented for the same symmetry site, which was chosen to assure the smallest deviation angles for the largest HF couplings. The lattice parameters were assumed to be as determined by Brown and Levy [17] in a neutron diffraction analysis: $a = 1.0868$ nm, $b = 0.8710$ nm, $c = 0.7761$ nm and $\beta = 102.97°$, where β denotes the angle between $<a>$ and $<c>$ axes. The $<a^*bc>$ orthogonal reference frame was chosen in accordance with previous work, where $<a^*>$ is perpendicular to $<b>$ and $<c>$. The chemical structure of the sucrose molecule and the labeling scheme are both shown in Fig. 1A.

Calculations were performed using the CP2K software package [18] and the BLYP exchange-correlation functional [19, 20]. To prevent interactions of the radical with its periodic images, a supercell doubled in the $<c>$ crystallographic direction ($<ab2c>$) was

2

used. Geometries were first optimized using the Gaussian and plane waves (GPW) dual basis set method [21] with a plane wave cutoff energy of 300 Ry, TZV2P GTH Gaussian basis sets [22] and GTH pseudopotentials [23, 24]. Then the obtained geometries were further refined on a higher level of theory: all-electron Gaussian and augmented plane waves (GAPW) [25] with an energy cutoff of 350 Ry and 6-311G** Gaussian basis sets [22, 26]. The HF tensors were calculated as described in Ref. 27 using the same level of theory as for the final geometry refinement — all-electron approach with 350 Ry cutoff and 6-311G** basis sets. To account for the spin-orbit and spin-other-orbit contributions erroneously described by effective potential methods [28], the **g** tensors were calculated by employing a scaling approximation proposed by Van Yperen-De Deyne et al. [29].

Temperature effects on the HF tensors were accounted for as described by Pauwels [15]. Calculated HF tensors were averaged over a sample of geometries obtained in an MD simulation run. In principle, the same method can be applied to the **g** tensor, but at this point in time it would be computationally too expensive. The MD calculations were performed using the canonical NVT ensemble, applying a canonical sampling through velocity rescaling thermostat [30] with a time constant of 25 fs. In total, more than 1 ps of dynamics at 110 K was simulated using a $\Delta t = 0.75$ fs time step.

3. Results and Discussion

Recently, single crystal and powder ENDOR and ENDOR-induced EPR characterization of the fourth stable radical allowed to determine the **g** tensor and 4 HF tensors. Two of these ($H_{\beta 1}$ and $H_{\beta 2}$) exhibit the typical characteristics of HF interactions of C-bound β protons. The third ($H_{\beta 3}$) and the fourth (H_{HO}) protons were respectively assigned to carbonyl and hydroxyl groups. Using semi-empirical theory and DFT calculations on an isolated molecular fragment, it was proposed that the fourth stable radical is a carbon-centered species surrounded by alkene ($-CH_2-R$), aldehyde ($-COH$) and hydroxyl ($-OH$) groups [13]. (This structure can be seen in the fragment in Fig. 1D.) Even though these constraints are insufficient to unambiguously determine the location of the unpaired electron in the molecule, the number of possible sites can be drastically reduced. In Ref. 13, only H-abstraction models were considered and two likely radical sites, i.e. C5 and C5', were proposed. If more complex models are permitted and the number of alterations is kept to a minimum, inspection of the sucrose molecule (Fig. 1A) reveals that all required chemical features could be accommodated not only around the C5 and C5' sites, but also around C2'. Possible models originating from these three sites were then further tested by DFT calculations as described above. In the course of the calculations (see Supporting Information), the C2' and C5 sites could be eliminated and a C5'-centered model was further explored.

The model of the radical that fits the experimental data best is presented in Fig. 1D. Calculated **g** and HF tensors are presented and compared to the corresponding experimental data in Table 1. The labeling of the protons in the pristine sucrose molecule is taken over for the calculated HF tensors. The $H_{\beta 1}$ HF interaction and the **g** tensor are reproduced very well: the principal directions deviate from the experimental values by $\sim 10°$ and the principal values possess the correct anisotropy, although they are slightly over- and

3

underestimated for the **g** and HF tensors, respectively. These are known shortcomings of DFT predictions [12, 15]. The direction of the largest principle value of H4'a, which lies along the H4'a–C5' direction, differs by only 4° from the corresponding one of $H_{\beta 1}$. The two smaller interactions with H4'b- and H6'-protons are reproduced rather well, although somewhat larger deviation angles (δ) with the experimental principal directions are noted. Finally, the principal values of the tensor assigned to HO5' are reproduced very well, but quite large δ values are observed. The temperature effects on the HF tensors were assessed by molecular dynamics (MD) simulations. The previously discussed trends did not change, although the correspondence for all tensors noticeably improved.

Causes of the remaining discrepancies were further explored by altering the hydroxyl groups in the vicinity of HO5' to affect the hydrogen bonding of the fragment molecule. All attempted changes either worsened the agreement of calculated tensors or resulted in unstable structures. It is possible that the mismatch associated with the HF tensor of HO5' is due to more substantial differences in conformations of neighboring molecules, which lie beyond the range accessible to the combined EPR/DFT approach. Regardless, the overall agreement is very good and cannot be coincidental, considering the number of available experimental tensors. Other locations for the same radical fragment in the sucrose lattice have been tested computationally and yielded considerable discrepancies with the experiment. The fact that no constraints were applied during the geometry optimization of the structure in Fig. 1D makes the identification even more convincing. This strongly suggests that the radical structure and its location in the lattice have now been identified.

The optimized radical structure in its environment is shown in Fig. 2. In order for this structure to be formed, the following alterations to the molecule are required, albeit not necessarily in this order and through distinct intermediate stages: a net H-abstraction from C5', cleavage of the O5'–C5' and C2'–C3' bonds, deoxygenation of C3', formation of a carbonyl group on C2' and a rearrangement of the C6' side arm, shown in Scheme 1. The result is a surprisingly complex structure of an allylic-type radical stabilized by hydrogen bonds in the crystal matrix. During RT irradiation [31], however, sufficient thermal energy is available for these various processes to occur. H-abstraction reactions are very common in the radiation chemistry of organic molecules and it was recently shown using MD simulations how hydrogen atoms can be removed through hydrogen bonds [32]. Ring opening radicals have so far not been observed in EPR studies of sucrose, but they were suggested in chromatographic studies of this carbohydrate [33], were predicted in the above mentioned MD study of rhamnose [32] and have been reported in β-D-fructose [34, 35]. Finally, fragmentation is known to occur in sucrose only through the rupturing of the glycosidic bond [11, 10], but there are no obvious obstacles preventing this from happening at other positions in the molecule. It seems from all of this that the resulting radical structure fits reasonably in the context of previous studies and illustrates the complexity of radiation damage to organic solids. It is also interesting to note that the identification of this radical may point to a symmetry in the radical composition of X-irradiated sucrose. Previous studies [10, 11] established that one of the stable radicals labeled as T1 is centered at C2' in the fructose unit (Fig. 1B) and that two distinct radicals with the same basic radical model — T2 and T3 — are formed in the glucose unit at C1 (Fig. 1C). Now, a second radical, labeled as T4 in Ref. 13 and identified in

4

Table 1: Comparison of the experimental **g** and HF tensors of the fourth stable radical species in X-irradiated sucrose to calculated tensors of the proposed model in the ground state and at 110 K (Fig. 1D).[a]

Tensor	g-value	δg^b	Iso^c	Aniso^c	δ^d	Iso^c	Aniso^c	δ^d
		Experiment^e						
g	2.0021	-0.3						
	2.0044	2.1						
	2.0064	4.1						
H$_{\beta1}$			80.1	-4.3				
				-1.5				
				5.8				
H$_{\beta2}$			36.2	-3.9				
				-2.4				
				6.3				
H$_{\beta3}$			-15.8	-8.1				
				-3.1				
				11.2				
H$_{HO}$			-7.1	-8.0				
				-6.5				
				14.5				
		DFT ($T = 0$ K)				*DFT+MD* ($T = 110$ K)		
g	2.0022	-0.1			12			
	2.0046	2.3			12			
	2.0067	4.4			4			
H4'a			75.9	-3.6	9	71.6	-3.5	5
				-2.4	9		-2.3	5
				6.0	4		5.8	2
H4'b			27.4	-3.9	18	31.2	-3.9	17
				-2.3	20		-2.2	18
				6.2	10		6.1	8
H6'			-13.2	-6.8	4	-13.5	-7.1	5
				-4.8	15		-4.5	9
				11.6	16		11.6	10
HO5'			-5.6	-8.5	18	-6.9	-8.3	15
				-6.1	45		-5.7	39
				14.6	41		14.1	37

[a]Complete tensors are available in Tables S4 and S5 in the Supporting Information. [b]Anisotropic g-values are presented as shifts from $g_e = 2.0023$ and are expressed in parts per thousand (ppt). [c]Principal values of the HF tensors are expressed in MHz. [d]Angles between the corresponding principal directions of experimental and calculated tensors are expressed in degrees. [e]Ref. 13.

this work, is also found to be located in the fructose unit. Experimentally estimated relative contributions of these four species [13] suggest that an equal share of stable paramagnetic radiation damage occurs in the two subunits of the sucrose molecule.
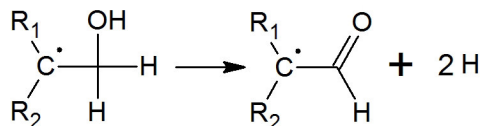
Scheme 1: Rearrangement of the C6' side arm into an aldehyde group by release of two H atoms.

Another important point to discuss is whether a possible precursor to this radical exists among primary or close-to-primary species, which can be created and trapped during low-temperature irradiations. A short summary of the subject is available in Ref. 16 and a detailed discussion can be found in Ref. 14. The latter contains data from a study of sucrose single crystals after irradiation at 80 K, where a promising candidate radical (N1) was reported. This species was tentatively identified as a net H-abstraction from the C5' site. Although the experimental data set was insufficient to elucidate the exact structure of this species, the strikingly good agreement of the data at hand strongly suggested that the site assignment was correct. It seems plausible that the N1 species could act as a precursor to the stable radical presented in Fig. 1D, but this cannot be said with certainty. It is possible that the the unpaired electron is first found on a neighboring site (C4' or C6') and then gets transferred to C5'. These matters should be further explored experimentally with annealing experiments after low temperature irradiation [14] and computationally with nudged elastic band simulations [36, 37, 38].

4. Conclusion

In conclusion, we have determined the radical model of the fourth stable radical species in X-irradiated sucrose. The final structure implies an H atom abstraction from the C5' site in the fructose unit, rupture of several bonds and considerable rearrangements of the entire molecule. This effectively breaks the molecule into two parts, resulting in two fragments suspended by hydrogen bonds in the crystal lattice. This identification reveals that the radiation damage in solids can be very complex and may reach the boundaries of conventional radiation chemistry intuition. It also shows that these problems can now be successfully handled by a synergy of high-resolution experimental techniques and sophisticated theoretical methods.

Appendix A. Supplementary Material

Supplementary data associated with this article can be found, in the online version.

References

[1] R. C. Rowe, P. J. Sheskey, W. G. Cook, M. E. Fenton (Eds.), Handbook of Pharmaceutical Excipients, 7th Edition, Pharmaceutical Press, London; Chicago, 2012.

[2] M. S. Holm, S. Saravanamurugan, E. Taarning, Conversion of Sugars to Lactic Acid Derivatives Using Heterogeneous Zeotype Catalysts, Science 328 (5978) (2010) 602–605. doi:10.1126/science.1183990.

[3] A. Studer, D. P. Curran, Catalysis of Radical Reactions: A Radical Chemistry Perspective, Angewandte Chemie International Edition 55 (1) (2016) 58–102. doi:10.1002/anie.201505090.

[4] G. Yang, C. Zhu, X. Zou, L. Zhou, Radicalization and Radical Catalysis of Biomass Sugars: Insights from First-principles Studies, Scientific Reports 6 (2016) 29711. doi:10.1038/srep29711.

[5] T. Nakajima, Sugar as an emergency populace dosimeter for radiation accidents, Health Physics 55 (6) (1988) 951–955.

[6] P. Fattibene, T. L. Duckworth, M. F. Desrosiers, Critical evaluation of the sugar-epr dosimetry system, Applied Radiation and Isotopes 47 (11) (1996) 1375–1379. doi:10.1016/S0969-8043(96)00254-0.

[7] Y. Karakirova, N. D. Yordanov, Sucrose as a dosimetric material for photon and heavy particle radiation: A review, Radiation Physics and Chemistry 110 (2015) 42–50. doi:10.1016/j.radphyschem.2015.01.014.

[8] D. Williams, J. E. Geusic, M. L. Wolfrom, L. J. McCab, Paramagnetic resonance study of irradiation damage in crystalline carbohydrates, Proceedings of the National Academy of Sciences 44 (11) (1958) 1128–1136.

[9] E. Sagstuen, A. Lund, O. Awadelkarim, M. Lindgren, J. Westerling, Free radicals in X-irradiated single crystals of sucrose: a reexamination, The Journal of Physical Chemistry 90 (22) (1986) 5584–5588. doi:10.1021/j100280a022.

[10] H. De Cooman, E. Pauwels, H. Vrielinck, E. Sagstuen, F. Callens, M. Waroquier, Identification and conformational study of stable radiation-induced defects in sucrose single crystals using density functional theory calculations of electron magnetic resonance parameters, The Journal of Physical Chemistry B 112 (24) (2008) 7298–7307. doi:10.1021/jp712004g.

[11] H. De Cooman, E. Pauwels, H. Vrielinck, E. Sagstuen, S. Van Doorslaer, F. Callens, M. Waroquier, ENDOR and HYSCORE analysis and DFT-assisted identification of the third major stable radical in sucrose single crystals X-irradiated at room temperature, Physical Chemistry Chemical Physics 11 (7) (2009) 1105–1114. doi:10.1039/b816641b.

[12] H. De Cooman, J. Keysabyl, J. Kusakovskij, A. Van Yperen-De Deyne, M. Waroquier, F. Callens, H. Vrielinck, Dominant stable radicals in irradiated sucrose: g tensors and contribution to the powder electron paramagnetic resonance spectrum, Journal of Physical Chemistry B 117 (24) (2013) 7169–7178. doi:10.1021/jp400053h.

[13] J. Kusakovskij, I. Caretti, S. V. Doorslaer, F. Callens, H. Vrielinck, Fourth stable radical species in X-irradiated solid-state sucrose, Physical Chemistry Chemical Physics 18 (16) (2016) 10983–10991. doi:10.1039/C6CP01118G.

[14] H. Vrielinck, H. De Cooman, F. Callens, E. Sagstuen, Radiation chemistry of solid-state carbohydrates using emr, in: A. Lund, M. Shiotani (Eds.), Applications of EPR in Radiation Research, Springer International Publishing, 2014, pp. 189–254.

[15] E. Pauwels, Uncovering Radiation Chemistry in the Solid State Through Periodic Density-Functional Calculations: Confrontation with Experimental Results and Beyond, in: A. Lund, M. Shiotani (Eds.), Applications of EPR in Radiation Research, Springer International Publishing, 2014, pp. 667–702.

[16] J. Kusakovskij, F. Callens, H. Vrielinck, EMR study and DFT-assisted identification of transient radicals in X-Irradiated crystalline sucrose, The Journal of Physical Chemistry B 119 (22) (2015) 6562–6570. doi:10.1021/acs.jpcb.5b02468.

7

[17] G. M. Brown, H. A. Levy, Further refinement of the structure of sucrose based on neutron-diffraction data, Acta Crystallographica Section B 29 (4) (1973) 790–797. doi:10.1107/S0567740873003353.

[18] G. Lippert, M. Parrinello, J. Hutter, A hybrid gaussian and plane wave density functional scheme, Molecular Physics 92 (3) (1997) 477–488. doi:10.1080/002689797170220.

[19] A. D. Becke, Density-functional exchange-energy approximation with correct asymptotic behavior, Physical Review A 38 (6) (1988) 3098–3100. doi:10.1103/PhysRevA.38.3098.

[20] C. Lee, W. Yang, R. G. Parr, Development of the colle-salvetti correlation-energy formula into a functional of the electron density, Physical Review B 37 (2) (1988) 785–789. doi:10.1103/PhysRevB.37.785.

[21] J. VandeVondele, M. Krack, F. Mohamed, M. Parrinello, T. Chassaing, J. Hutter, Quickstep: Fast and accurate density functional calculations using a mixed gaussian and plane waves approach, Computer Physics Communications 167 (2) (2005) 103–128. doi:10.1016/j.cpc.2004.12.014.

[22] R. Krishnan, J. S. Binkley, R. Seeger, J. A. Pople, Self-consistent molecular orbital methods. xx. a basis set for correlated wave functions, The Journal of Chemical Physics 72 (1) (1980) 650–654. doi:10.1063/1.438955.

[23] S. Goedecker, M. Teter, J. Hutter, Separable dual-space gaussian pseudopotentials, Physical Review B 54 (3) (1996) 1703–1710. doi:10.1103/PhysRevB.54.1703.

[24] C. Hartwigsen, S. Goedecker, J. Hutter, Relativistic separable dual-space gaussian pseudopotentials from h to rn, Physical Review B 58 (7) (1998) 3641–3662. doi:10.1103/PhysRevB.58.3641.

[25] G. Lippert, J. Hutter, M. Parrinello, The gaussian and augmented-plane-wave density functional method for ab initio molecular dynamics simulations, Theoretical Chemistry Accounts 103 (2) (1999) 124–140. doi:10.1007/s002140050523.

[26] A. D. McLean, G. S. Chandler, Contracted gaussian basis sets for molecular calculations. i. second row atoms, z=11–18, The Journal of Chemical Physics 72 (10) (1980) 5639–5648. doi:10.1063/1.438980.

[27] R. Declerck, E. Pauwels, V. Van Speybroeck, M. Waroquier, First-principles calculations of hyperfine parameters with the gaussian and augmented-plane-wave method: Application to radicals embedded in a crystalline environment, Physical Review B 74 (24) (2006) 245103. doi:10.1103/PhysRevB.74.245103.

[28] F. Neese, Efficient and accurate approximations to the molecular spin-orbit coupling operator and their use in molecular g-tensor calculations, The Journal of Chemical Physics 122 (3) (2005) 034107. doi:10.1063/1.1829047.

[29] A. Van Yperen-De Deyne, E. Pauwels, V. Van Speybroeck, M. Waroquier, Accurate spin-orbit and spin-other-orbit contributions to the g-tensor for transition metal containing systems, Physical Chemistry Chemical Physics 14 (30) (2012) 10690–10704. doi:10.1039/C2CP41086A.

[30] G. Bussi, D. Donadio, M. Parrinello, Canonical sampling through velocity rescaling, The Journal of Chemical Physics 126 (1) (2007) 014101.

[31] H. Vrielinck, H. De Cooman, Y. Karakirova, N. D. Yordanov, F. Callens, Early-stage evolution of the epr spectrum of crystalline sucrose at room temperature after high-dose x irradiation, Radiation research 172 (2) (2009) 226–233. doi:10.1667/RR1746.1.

[32] S. G. Aalbergsjø, E. Pauwels, A. Van Yperen-De Deyne, V. V. Speybroeck, E. Sagstuen, Automated generation of radical species in crystalline carbohydrate using ab initio MD simulations, Physical Chemistry Chemical Physics 16 (32) (2014) 17196–17205.

[33] D. Peshev, R. Vergauwen, A. Moglia, É. Hideg, W. Van den Ende, Towards understanding vacuolar antioxidant mechanisms: a role for fructans?, Journal of Experimental Botany 64 (4) (2013) 1025–1038.

[34] M. A. Tarpan, H. Vrielinck, H. D. Cooman, F. Callens, Determination of the g Tensors for the Dominant Stable Radicals in X-Irradiated β-d-Fructose Single Crystals, The Journal of Physical Chemistry A 113 (28) (2009) 7994–8000.

[35] M. A. Tarpan, E. Pauwels, H. Vrielinck, M. Waroquier, F. Callens, Electron Magnetic Resonance and Density Functional Theory Study of Room Temperature X-Irradiated β-d-Fructose Single Crystals, The Journal of Physical Chemistry A 114 (47) (2010) 12417–12426.

[36] G. Henkelman, H. Jónsson, Improved tangent estimate in the nudged elastic band method for finding minimum energy paths and saddle points, The Journal of Chemical Physics 113 (22) (2000) 9978–9985. doi:10.1063/1.1323224.

[37] G. Henkelman, B. P. Uberuaga, H. Jónsson, A climbing image nudged elastic band method for finding saddle points and minimum energy paths, The Journal of Chemical Physics 113 (22) (2000) 9901–9904. doi:10.1063/1.1329672.

[38] E. Pauwels, H. D. Cooman, M. Waroquier, E. O. Hole, E. Sagstuen, Solved? The reductive radiation chemistry of alanine, Physical Chemistry Chemical Physics 16 (6) (2014) 2475–2482. doi:10.1039/C3CP54441A.
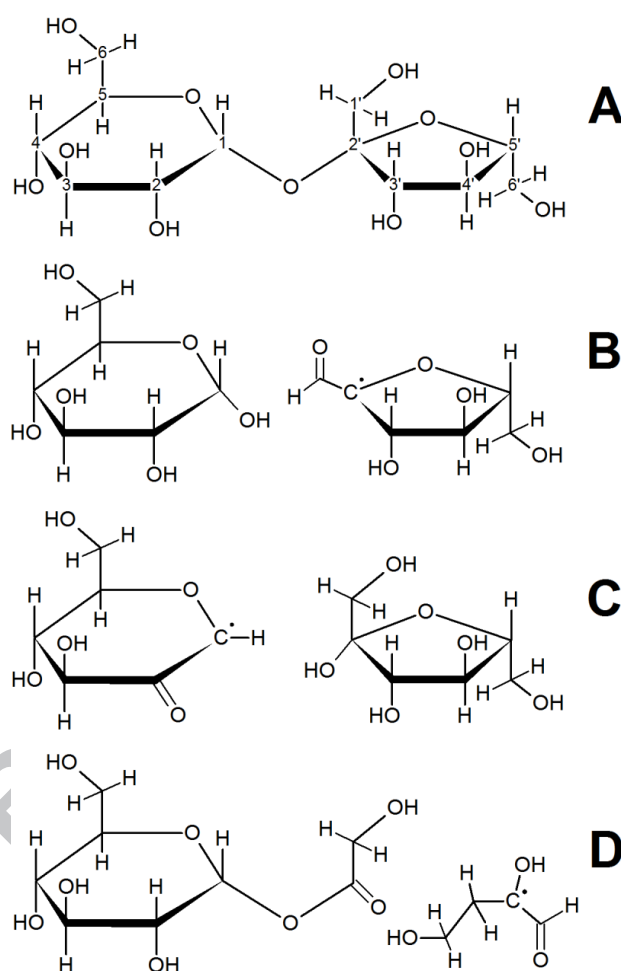
Figure 1: Chemical structures of a pristine sucrose molecule (A), known stable radical species (B — T1, C — T2/T3) and the proposed model for the fourth as yet unknown species (D). Throughout this work, carbon atoms are numbered as shown in panel A: hydrogen and oxygen atoms are labeled according to the carbon to which they are bound, with the exception of hydroxyl hydrogen atoms, which are numbered according to the oxygen to which they are bound. The glycosidic, the glucose and the fructose ring oxygen atoms are labeled as O1, O5 and O5', respectively.
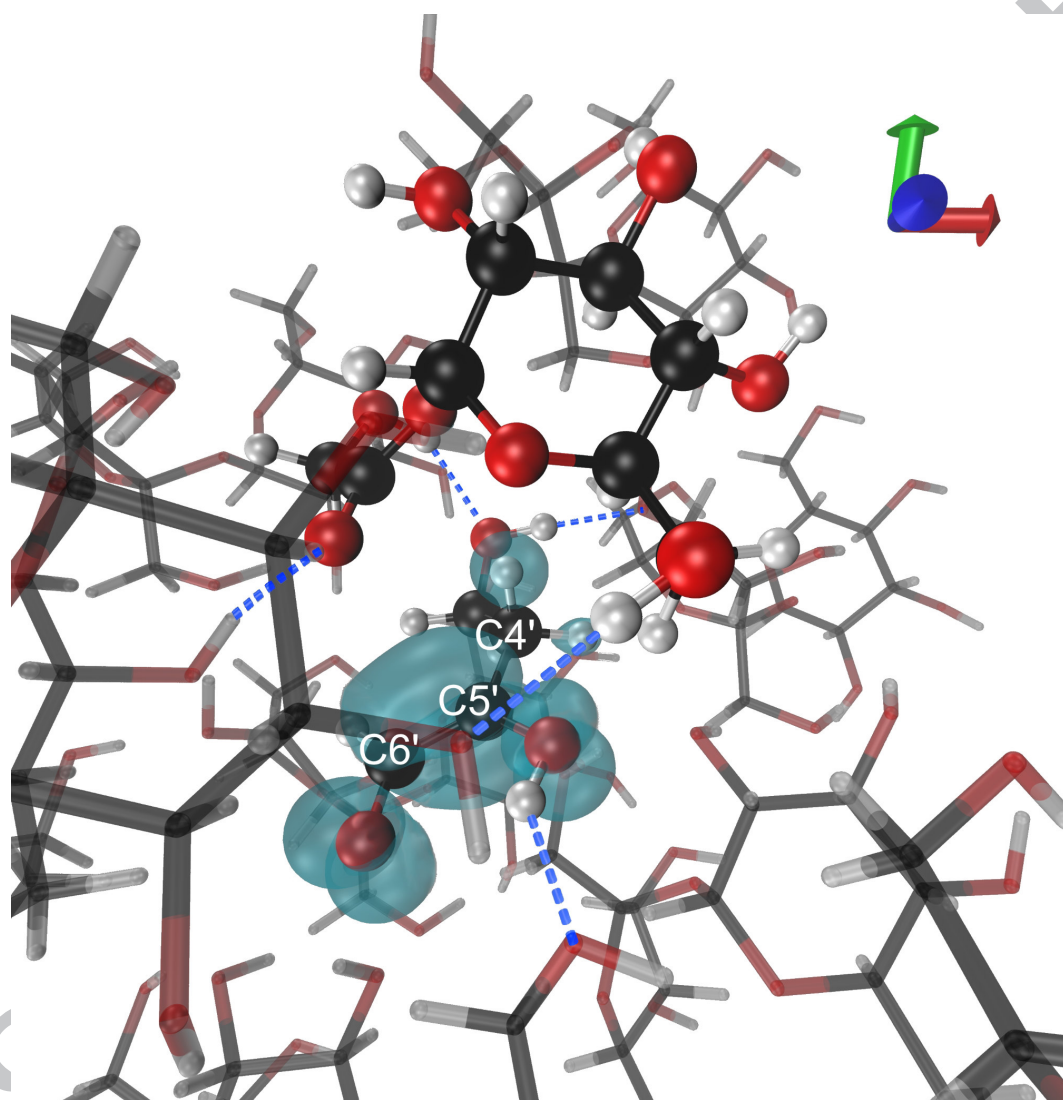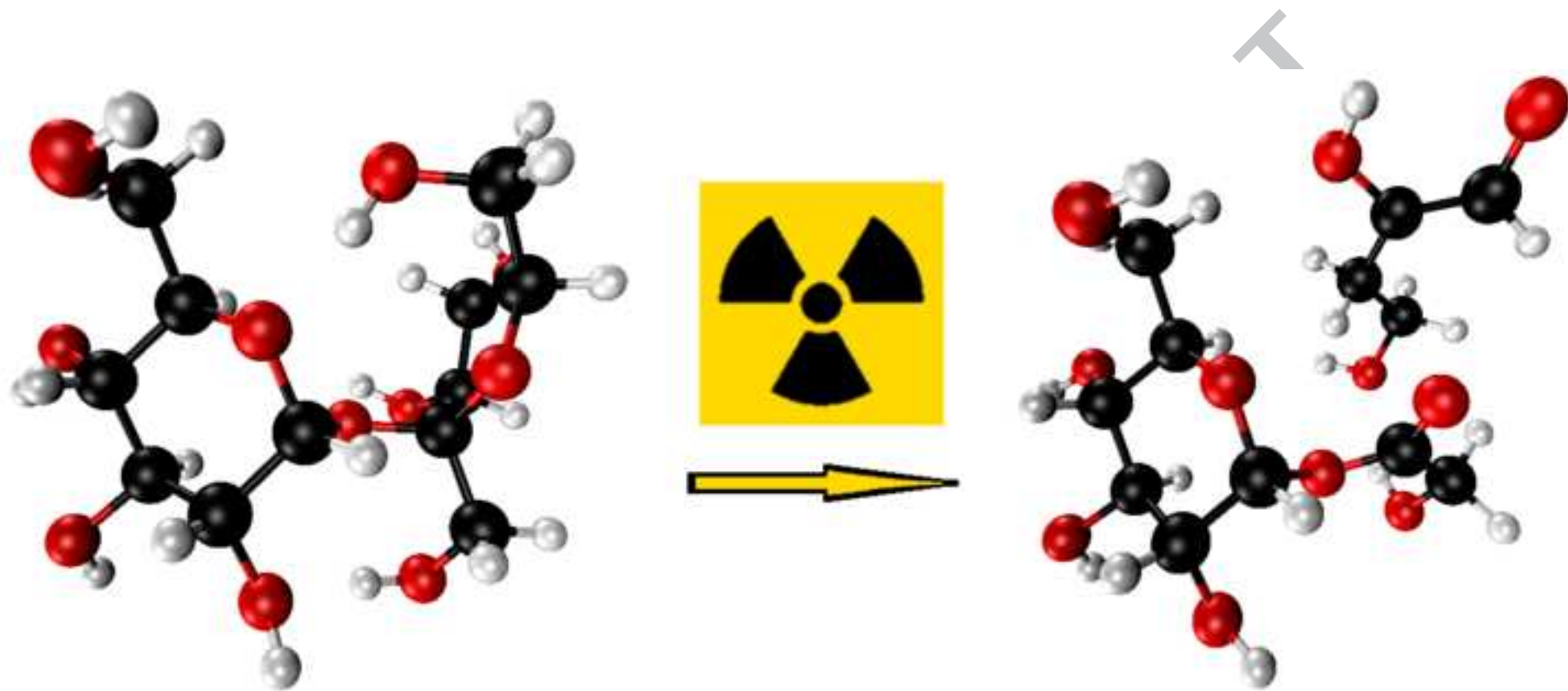
Figure 2: Optimized structure of the model of the fourth stable radical species in X-irradiated sucrose (Fig. 1D). The molecule containing the radical center is represented by solid balls and sticks, the nearest neighbors — by semitransparent tubes, the hydrogen bonds — by dashed blue lines. Directions of the reference frame are shown in the top right corner and are color coded as red for $<a^*>$, green for $<b>$ and blue for $<c>$. The spin density distribution is visualized by means of a spin density isosurface ($\rho = 0.002$).

Graphical Abstract (pictogram)